

IPO: Iterative Preference Optimization for Text-to-Video Generation

Xiaomeng Yang^{2*} Zhiyu Tan^{1,2*} Hao Li^{1,2†}

¹ Fudan University, ² Shanghai Academy of Artificial Intelligence for Science

Abstract

Video foundation models have achieved significant advancement with the help of network upgrade as well as model scale-up. However, they are still hard to meet requirements of applications due to unsatisfied generation quality. To solve this problem, we propose to align video foundation models with human preferences from the perspective of post-training in this paper. Consequently, we introduce an Iterative Preference Optimization strategy to enhance generated video quality by incorporating human feedback. Specifically, IPO exploits a critic model to justify video generations for pairwise ranking as in Direct Preference Optimization or point-wise scoring as in Kahneman-Tversky Optimization. Given this, IPO optimizes video foundation models with guidance of signals from preference feedback, which helps improve generated video quality in subject consistency, motion smoothness and aesthetic quality, etc. In addition, IPO incorporates the critic model with the multi-modality large language model, which enables it to automatically assign preference labels without need of retraining or relabeling. In this way, IPO can efficiently perform multi-round preference optimization in an iterative manner, without the need of tediously manual labeling. Comprehensive experiments demonstrate that the proposed IPO can effectively improve the video generation quality of a pretrained model and help a model with only 2B parameters surpass the one with 5B parameters. Besides, IPO achieves new state-of-the-art performance on VBench benchmark. The source code and model checkpoints, along with implementation details and resources, are openly available at [this GitHub repository](#).

1. Introduction

Text-to-video generation has drawn lots of attention due to its great potentials in movie products, video effects and user-generated contents, etc. Recent works [2, 10, 16] introduce the Transformer architecture into diffusion models and improve the video generation quality by simply scaling up the parameter size, e.g., CogVideoX-5B [43], Mochi-10B [35] and HunyuanVideo-13B [15]. Although achieving

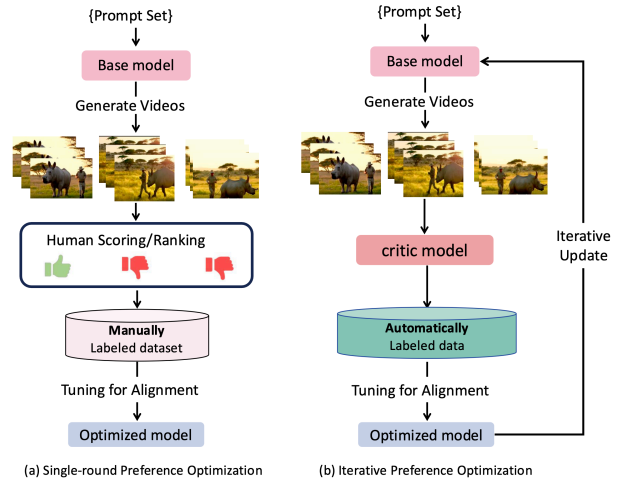


Figure 1. Comparison of (a) traditional single-round preference optimization and (b) the proposed Iterative Preference Optimization for aligning video foundation model with human feedback. IPO introduces a critic model to automatically labeling video data without need of tedious manual efforts, making iterative update possible in an efficient way.

impressive performance, they still face challenges for generating user-satisfied videos with consistent subject, smooth motion and high-aesthetic picture. In addition, their large model sizes make them slow to produce videos. These drawbacks limit their applications in practice.

To align generation results with human preference, post-training techniques have shown their effectiveness in fields of Large Language Models (LLMs) and Text-to-Image models (T2Is). For instance, Direct Preference Optimization (DPO) [27] exploits pairwise ranked data to make LLMs know the language style liked by human. While Kahneman-Tversky Optimization (KTO) [7] uses pointwisely binary data to reinforce T2Is to learn how to maximumly align the objective with human expectation. These techniques promote generative models to derive user-satisfied contents and give us inspiration for improving video generation models.

Thus, we propose to align Text-to-Video models (T2Vs) with human preference from the perspective of post-training in this paper. In particular, we present the Iterative Preference Optimization (IPO) framework for enhancing T2Vs.

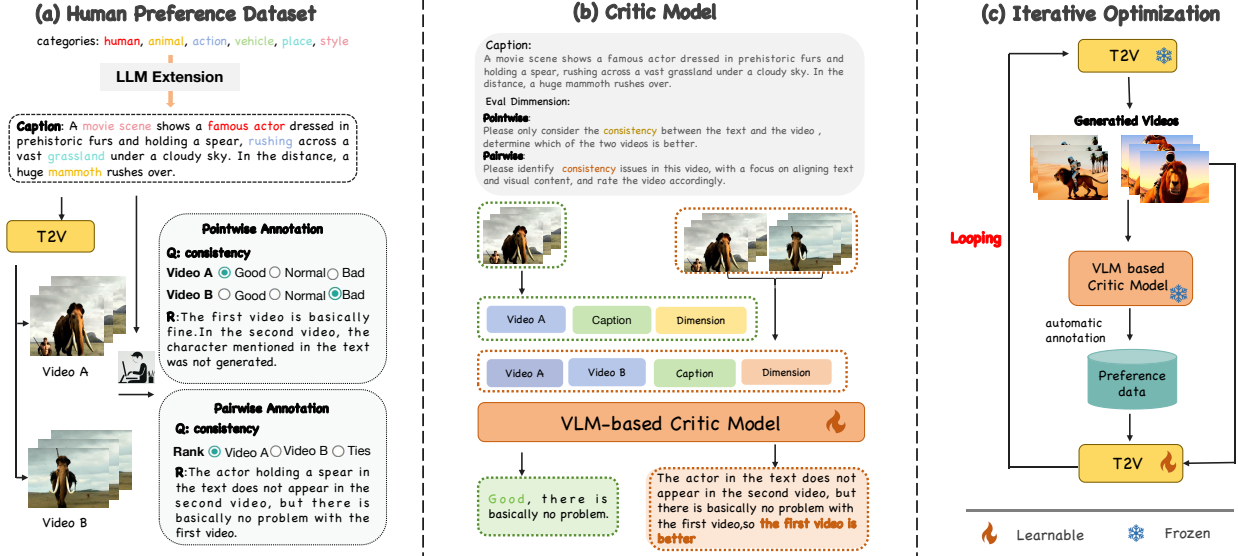


Figure 2. The overview of our proposed Iterative Preference Optimization framework. IPO consists of three major parts: (a) Human Preference Dataset. It is used to train a critic model. This dataset only requires one-round manual annotation without need of relabeling in the iterative framework; (b) Critic Model. It is learned to automatically annotate generated videos with preference labels, which help eliminate tedious manual efforts for multi-round optimization; (c) Iterative Optimization. It incorporates the critical model to iteratively optimize video foundation model. In this way, IPO can efficiently tune the base model to align with human preference and enhance generation ability in aspects of subject consistency, motion smoothness and aesthetic quality, etc. **Best viewed in 2x zoom.**

IPO introduces preference priors for finetuning T2Vs in the form of reinforcement learning, which considers subject consistency, motion smoothness and aesthetic quality, etc. This leads to improved video generations that are well aligned with human preference. In addition, as show in Fig. 1, difference from prior single-round methods, IPO adopts a multi-round optimization strategy to reinforce T2Vs in an iterative manner, which strengthens the models continuously. In this way, IPO can effectively improve T2Vs without need of large-scale dataset and expensive supervised finetuning.

Specifically, IPO consists of three core parts as shown Fig. 2: the preference dataset, the critic model and the iterative learning framework. IPO first collects a preference dataset for training the critic model. To get this dataset, IPO predefines several categories, including human, animal, action, etc. Then, IPO randomly combines these categories and uses LLM to extend them as prompts for generating videos with T2V models. Given these videos, IPO manually annotates them with two kinds of labels: one is pairwise ranking label that depicts preference comparison of two videos; another is pointwise scoring label that describes video quality as good or bad in a binary manner. After collecting the preference dataset, IPO uses it to train a critic model for justifying the quality of input videos. Concretely, IPO exploits Multi-modality Large Language Models (MLLMs) to achieve the above goal considering their powerful capability for recognizing video contents. In addition, IPO combines instruction-tuning to learn the critic

model, making it able to generate pairwise and pointwise labels with different prompts. Given the critic model, IPO plays as a plugin for preference optimization of T2Vs without requirements of retraining or relabeling. For a specific T2V model, IPO can either use Diffusion-DPO [36] with pairwise ranking data or Diffusion-KTO [18] with pointwise scoring data. In addition, IPO adopts the critic model for automatically labeling videos from the reinforced T2Vs, which can be used as prior information for further improving T2Vs. In the iterative way, IPO can consistently improve T2Vs for generating high-quality videos.

Comprehensive experiments on benchmark VBench demonstrate that the proposed IPO can effectively and efficiently reinforce T2Vs to produce user-satisfied videos with consistent subject, smooth motion as well as high-aesthetic quality. In addition, given CogVideoX as the video foundation model, IPO can improve a 2B model to surpass the 5B counterpart. Our contributions can be summarise into three folds: First, we introduce a new preference optimization framework into text-to-video generation, which well align generations with human preference. Second, we present a novel iterative post-training framework for enhancing foundation models in a multi-round manner, differing from prior single-round methods. Third, we set new state-of-the-art on the benchmark VBench both in quantity and quality. To advance future researches in the area of video generation, we will release the preference dataset, the codes, the critic models as well as T2V models.

2. Related Work

Text-to-video generation Recent advances in video generation have been largely driven by diffusion models [11, 31, 32, 46], achieving remarkable improvements in diversity, fidelity, and quality [4, 6, 13, 20, 29, 38, 40]. Scaling model size and training data further enhance performance [12, 30, 39]. In Text-to-Video (T2V) generation, pre-training from scratch requires substantial computational resources and large-scale datasets [2, 8, 15, 16, 22]. Current methods [1, 9, 37] extend text-to-image models by incorporating spatial and temporal attention modules, often using joint image-video training [23], with [9] proposing a plug-and-play temporal module for personalized image models. State-of-the-art pixel quality and temporal consistency have been achieved by [3, 47], while diffusion models based on the DiT structure [2, 3, 43] enhance spatiotemporal coherence and scalability, highlighting the potential of Transformer-based architectures. Despite of their success, they still cannot meet requirements in real scenarios due to lack of alignment with human preference.

Post-training for human preference alignment Post-training is a common technique exploited in Large Language Models (LLMs) [24, 28, 50]. Reinforcement Learning from Human Feedback (RLHF) [24] learns a reward function from comparison data to align the policy model. Rank Responses for Human Feedback (RRHF) [45] extends supervised fine-tuning, while Sequence Likelihood Calibration (SLiC) [49] leverages offline RL data. Direct Preference Optimization (DPO) [27] improves stability and efficiency by directly optimizing human preference data, and Kahneman-Tversky Optimization (KTO) [7] aligns models via a prospect-theoretic approach. Rejection Sampling Optimization (RSO) [21] enhances alignment using statistical rejection sampling. Prior works have introduced this technique into enhancement of image foundation models, such as [5, 25, 41]. Diffusion-DPO [36] extends DPO for diffusion models, optimizing model likelihood, while Diffusion-KTO [18] maximizes expected human utility without costly pairwise preference data. The usage of post-training in video generation is still rare. Current works mainly focus on the design of reward models. [44] introduced a temporal decaying reward (TAR) mechanism, prioritizing central frames for stable and coherent video generation. Meanwhile, [17] optimized ordinary differential equation (ODE) solvers by exploring energy function designs, enhancing T2V training through motion prior extraction. VADER [26] fine-tunes video diffusion models using reward model gradients and pre-trained vision models, achieving strong generalization even for unseen cues, thereby improving T2V adaptability and performance. However, the above strategies can only achieve minor improvements and not fully explore the potential of post-training.

3. METHOD

The proposed Iterative Preference Optimization framework consists of three major parts: (1) A human preference dataset for training critic model; (2) A critic model for automatically labeling generated videos; (3) An iterative optimization process for enhancing the base text-to-video models. Fig. 2 illustrates the whole pipeline of IPO. We will explain details of each part in the following sections.

3.1. Human Preference Dataset

Video-text Collection The generated video dataset is created using the CogVideoX-2B model [43]. We generate diverse prompts covering various character types, which are then combined and refined using the Qwen2.5 [42]. To increase diversity, we adjust parameters like temperature, top-k, and top-p. As shown in Fig. 3, the dataset includes over ten categories, such as Human, Architecture, Vehicles, and Animals, as well as more than ten different actions of human and animal. For each prompt, the video generation model produces four variants with different random seeds. The dataset is iteratively expanded through an optimized re-generation strategy to improve preference alignment.

Human Annotation When aligning human feedback, we focus on three dimensions, inspired by the text-to-image evaluation work Evalalign [34]: consistency between text and video, video faithfulness, and additional motion smoothness. To capture human preferences, we employ two annotation methods: **Pairwise Ranking** and **Pointwise Scoring**. For pairwise ranking, annotators are shown two videos generated from the same prompt and asked to evaluate them based on predefined criteria. They are required to: (1) provide detailed natural language feedback, and (2) identify specific quality issues in each video. The annotated comparisons are then organized to create training samples.

$$\left\{ \begin{array}{l} \langle \text{Video1} \rangle, \langle \text{Video2} \rangle, \text{Question}, \\ \text{Evaluation Dimension}, \\ \text{Ranking Answer, Reason} \end{array} \right\}$$

For pointwise scoring, each video is assessed across three dimensions, with scores categorized into three levels: **Good**, **Normal**, and **Poor**. Similar to the ranking process, annotators provide detailed justifications for their scores to ensure transparency and consistency. The annotated evaluations are then organized to create training samples.

$$\left\{ \begin{array}{l} \langle \text{Video} \rangle, \text{Question}, \\ \text{Evaluation Dimension}, \\ \text{Scoring Answer, Reason} \end{array} \right\}$$

Each dataset is annotated by at least three individuals. The final annotation is determined through voting, selecting the one with the highest consistency among reviewers.

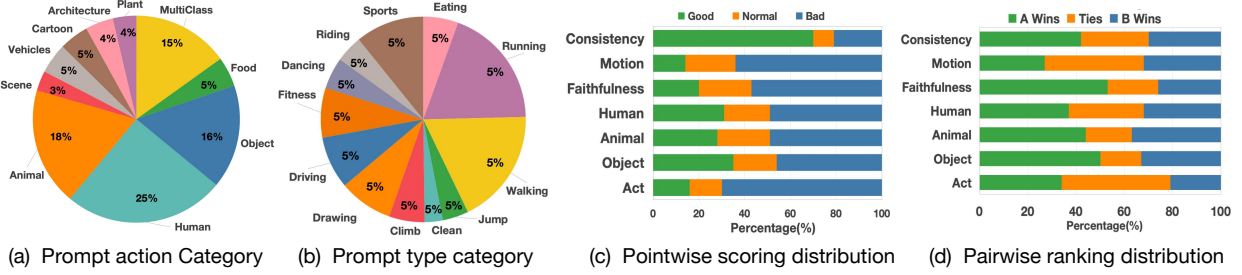


Figure 3. The distribution statistics of Human Preference Dataset on prompts in (a) and (b) as well as scoring/ranking in (c) and (d).

3.2. Critic Model Training

Large Visual-Language Models (VLMs) exhibit strong generalization across diverse tasks due to pre-training on extensive multimodal data. Their capability to capture complex text-image relationships makes them well-suited for critic modeling, where alignment with human preferences is crucial. Leveraging VLMs as critic models enhances video generation by improving preference predictions through their robust generalization ability.

Fig. 2 illustrates our supervised fine-tuning process. The training starts by passing video frames through an image encoder to extract image tokens. These tokens, together with the textual caption, question, and answer, are then fed into a pre-trained Visual-Language Model (VLM). Formally, each training sample consists of a triplet: **multimodal input** M , which includes both the video and its corresponding textual description; **question** Q ; and **answer** A .

The optimization objective is derived from the autoregressive loss function commonly used in LLM training, but applied specifically to the answer as:

$$L(\phi) = - \sum_{i=1}^N \log p(A_i | Q, M, A_{<i}; \phi), \quad (1)$$

where N is the length of the ground-truth answer. This loss encourages the model to get answers that align with provided questions and multimodal context. Depending on the method, the model receives different inputs. In the **pointwise** case, it evaluates a single video-text pair. In the **pairwise** case, it compares two pairs to determine which aligns better with the text. The optimization focuses on individual quality in pointwise and relative comparison in pairwise.

3.3. T2V Alignment

3.3.1. Alignment Optimization

In Reinforcement Learning with Human Feedback (RLHF), the primary objective is to optimize the model to maximize the expected reward given context c . This is achieved by incorporating a regularization term that penalizes deviations from a reference distribution, ensuring the optimized model remains consistent with prior knowledge or previously trained models. The optimization objective is as:

$$\max_{\pi_{\theta}} \mathbb{E}_{x_0 \sim \pi_{\theta}(x_0|c)} \left[r(x_0, c) - \beta \log \frac{\pi_{\theta}(x_0|c)}{\pi_{ref}(x_0|c)} \right], \quad (2)$$

where $r(x_0, c)$ denotes the reward associated with a state x_0 given context c , $\pi_{\theta}(x_0|c)$ is the policy of the model parameterized by θ , and $\pi_{ref}(x_0|c)$ is the reference policy. The hyperparameter β controls the strength of the regularization, typically set as a fixed constant. This objective function aims to balance reward maximization with regularization, which prevents the model from straying too far from the reference distribution, ensuring stability and generalization [48]. And the loss function for the policy $\pi_{\theta}(\cdot|c)$ is formulated in terms of the expected value over the reward and the KL-divergence penalty as following:

$$\mathbb{E}_{x_0 \sim \pi_{\theta}(x_0|c)} \left[-r(x_0, c) - \beta \log \frac{\pi_{ref}(x_0|c)}{\pi_{\theta}(x_0|c)} \right] = \beta \text{KL} \left(\pi_{\theta}(x_0|c) \parallel \pi_{ref}(x_0|c) \exp \left(\frac{1}{\beta} r(x_0, c) \right) \right), \quad (3)$$

Minimizing this loss leads to optimal policy $\pi^*(x_0|c)$ as:

$$\pi^*(x_0|c) \propto \pi_0(x_0|c) \exp \left(\frac{1}{\beta} r(x_0, c) \right), \quad (4)$$

This aligns with Direct Preference Optimization (DPO) [27] that translates the optimization goal into training the optimal policy $\pi^*(x_0|c)$. The key advantage of this formulation is that it incorporates both reward maximization and regularization into a unified framework, thereby enabling robust learning. To improve the model’s alignment with human feedback and output quality, we incorporate real-world data into the alignment training process. By using authentic, human-generated examples, the model learns to reduce hallucinations and better align with human preferences. This also enhances the model’s robustness and generalization, preventing training divergence and ensuring reliable performance in diverse real-world tasks.

3.3.2. Pointwise Optimization

For pointwise preference alignment, we adopt Diffusion-KTO [7]. Unlike traditional preference-based methods, KTO optimizes a nonlinear utility function using binary-labeled data, making it particularly sensitive to negative samples. This approach avoids the need for explicit preference pairs and introduces human-aware loss functions.

In Diffusion-KTO, the utility of an action is computed relative to a reference point Q_{ref} , defined as the KL divergence between the learned policy π_{θ} and the reference pol-

icy π_{ref} . The optimization objective is:

$$L_{\text{kto}}(\theta) = \max_{\pi_{\theta}} \mathbb{E}_{x_0 \sim \mathcal{D}, t \sim \text{Uniform}(0, T)} [U(w(x_0)(\beta \log \frac{\pi_{\theta}(x_{t-1}|x_t)}{\pi_{\text{ref}}(x_{t-1}|x_t)} - Q_{\text{ref}}))], \quad (5)$$

where $w(x_0) = \pm 1$ indicates whether a state x_0 is desirable or undesirable. The reference point Q_{ref} is defined as:

$$Q_{\text{ref}} = \beta \mathbb{D}_{\text{KL}}[\pi_{\theta}(a|s) || \pi_{\text{ref}}(a|s)]. \quad (6)$$

This adaptive reference mechanism allows Diffusion-KTO to calibrate the policy toward human-aligned decision-making. To optimize the policy, we use the loss function from Eq. 5. A challenge in KTO training is estimating the average reward Q , which becomes unstable with small batch sizes. To mitigate this, we set the batch size as 128 for stable Q estimation. To further improve stability and generalization, we incorporate real-world data from the VidGen-1M dataset [33]. We add a negative log-likelihood (NLL) loss term on real samples to regularize the model and prevent divergence from natural video distributions. The final training objective is:

$$\mathcal{L}(\theta) = L_{\text{kto}}(\theta) + \lambda \cdot \mathbb{E}_{(y,x) \sim \mathcal{D}^{\text{real}}} [-\log p_{\theta}(y|x)], \quad (7)$$

where λ controls the weight of real data regularization. This hybrid approach balances the model’s utility maximization with adherence to real-world video distributions, enhancing its alignment with human preferences.

3.3.3. Pairwise Optimization

For pairwise preference alignment, we adopt Diffusion-DPO [36], an extension of Direct Preference Optimization (DPO) [27] to diffusion models. Diffusion-DPO utilizes inverse decomposition to replace the standard policy π_{θ} and reference policy π_{ref} , enabling efficient preference optimization within the diffusion framework.

In Diffusion-DPO, the forward process $q(x_{1:T}|x_0)$ approximates the reverse process $p_{\theta}(x_{1:T}|x_0)$, redefining data likelihood in diffusion models. This leads to a loss function that facilitates robust preference optimization. The objective function for Diffusion-DPO is as:

$$L_{\text{dpo}}(\theta) = -\mathbb{E}_{(x_0^w, x_0^l) \sim \mathcal{D}, t \sim \mathcal{U}(0, T), x_t^w \sim q(x_t^w|x_0^w), x_t^l \sim q(x_t^l|x_0^l)} \log \sigma \left(-\beta T \omega(\lambda_t) \left(\|\epsilon^w - \epsilon_{\theta}(x_t^w, t)\|_2^2 - \|\epsilon^w - \epsilon_{\text{ref}}(x_t^w, t)\|_2^2 - \left(\|\epsilon^l - \epsilon_{\theta}(x_t^l, t)\|_2^2 - \|\epsilon^l - \epsilon_{\text{ref}}(x_t^l, t)\|_2^2 \right) \right) \right), \quad (8)$$

where x^w denotes the preferred sample, x^l the rejected sample, and $\omega(\lambda_t)$ is a weighting function [11, 14, 27].

During training, we use a selective sampling strategy to construct high-quality preference pairs by selecting the highest-ranked (preferred) and lowest-ranked (rejected) samples based on critic model evaluations. This ensures clearer preference distinctions and enhances learning. These pairs (y^w, y^l) form the final training data.

The optimization objective combines the Diffusion-DPO loss with two auxiliary negative log-likelihood (NLL) terms. The first, weighted by $\lambda_1=0.2$, regularizes the preferred samples to align with human preferences. The second, weighted by $\lambda_2=0.1$, anchors the model to real video distributions to prevent overfitting. The final loss is:

$$\begin{aligned} \mathcal{L}(\theta) = L_{\text{dpo}}(\theta) &+ \lambda_1 \cdot \mathbb{E}_{(y,x) \sim \mathcal{D}^{\text{sample}}} [-\log p_{\theta}(y^w|x)] \\ &+ \lambda_2 \cdot \mathbb{E}_{(y,x) \sim \mathcal{D}^{\text{real}}} [-\log p_{\theta}(y|x)], \end{aligned} \quad (9)$$

where $\mathcal{D}^{\text{sample}}$ represents the set of preference pairs derived from the critic model’s evaluation, and $\mathcal{D}^{\text{real}}$ denotes the real video data used for regularization.

3.3.4. Iterative Optimization

Iterative optimization is advantageous for complex tasks like preference alignment in reinforcement learning. Rather than approximating the optimal policy π_{θ} in a single step, which is computationally challenging, it decomposes the problem into manageable stages. This stepwise refinement enables incremental improvements, progressively aligning the model with human preferences in a more efficient and controlled manner. A key benefit of iterative optimization is that it enables more stable training. Rather than attempting to directly approximate the reference distribution $\pi_{\text{ref}} \exp\left(\frac{1}{\beta} r(x_0, c)\right)$ in a single step, the process proceeds in multiple stages. In each iteration, we approximate the distribution using the following formula:

$$\pi_{\text{ref}}^{(k)} = \pi_{\text{ref}}^{(k-1)} \exp\left(\frac{r^k}{\beta_k}\right), \quad (10)$$

where, r^k denotes the reward function at the k -th iteration, and β_k is a hyperparameter controlling the optimization rate at each stage. We initialize $r^0 = 0$ to start with a neutral reward function. As iterations progress, the reward function is refined, guiding the model toward an optimal policy.

Iterative refinement improves training control, enabling the model to gradually align with human feedback while avoiding early overfitting or divergence. By utilizing intermediate distributions at each stage, the method accommodates more complex feedback signals, leading to a more robust model that generalizes well across diverse real-world scenarios. Additionally, iterative optimization mitigates issues like catastrophic forgetting and instability, which can occur when attempting to approximate the optimal policy in a single step. Each iteration builds on the previous one, ensuring stable and reliable convergence toward the target policy. In this way, iterative preference optimization (IPO) enhances preference-based optimization by providing better training control, faster convergence, and improved generalization, making it a valuable tool for optimizing policies based on human feedback.



An astronaut with a red stripe on their suit is astride a powerful lion on a dune overlooking a desert oasis. The lion's eyes are fierce as it surveys the landscape. The astronaut has a canteen attached to their belt, hoping to find water soon. The palm trees of the oasis sway in the breeze, offering a promise of relief.



A director, dressed in a dark blazer and casual jeans, sits at a modern desk cluttered with scripts and notes. He types intently on a sleek laptop, his brow furrowed in concentration. The room is dimly lit by a single desk lamp, casting a warm glow over his focused expression. Behind him, a large window frames a city skyline at dusk, adding a sense of urgency and creativity to the scene.



A woman sits in a cozy, well-lit room, her hands deftly working a long, creamy white scarf. She wears a warm, olive-green sweater and a gentle smile, her eyes focused on the intricate pattern of her knitting. The soft, natural light streaming through a nearby window highlights the texture of the yarn and the calm, serene atmosphere of the space. Her concentration and skill are evident as she effortlessly manipulates the needles, creating a beautiful, handmade scarf.



An actor dressed in rugged, casual attire, including a dark jacket, jeans, and hiking boots, walks alongside a dingo in a natural, wooded setting. The dingo, with its distinctive reddish-brown fur and alert eyes, moves gracefully beside the actor, who looks calm and engaged. The background features lush greenery and dappled sunlight filtering through the trees, creating a serene and harmonious atmosphere. The actor and the dingo walk in sync, their bond evident in their synchronized steps and mutual awareness of each other.

Figure 4. Qualitative Comparison of our proposed IPO model and the baseline CogVideoX-2B model. We can see IPO improves the baseline in the aspects of prompt following (the 1st line), aesthetic quality (the 2nd line), subject consistency (the 3rd line) and motion smoothness (the 4th line). This demonstrates the effectiveness of our IPO for enhancing the generation capability of video found models. Additional visualization results are available in the supplementary materials.

Method	Quality Score	Semantic Score	Total Score
CogVideoX-2B	82.18	75.83	80.91
CogVideoX-5B	82.75	77.04	81.61
CogVideoX-2B-IPO-3	83.92	78.00	82.74

Table 1. Comparison of IPO with baselines CogVideoX models.

Models	Subject Consist.	Motion Smooth	Aesthetic Quality
CogVideoX-2B	96.78	97.73	60.82
w/o real data sft	96.56	97.81	61.25
w/ real data sft	96.77	97.84	61.55

Table 2. Ablation studies on effects of real data for finetuning IPO.

4. Experiments

4.1. Experimental Setup

4.1.1. Critic Model Training

To unify paired data sorting and individual video scoring, we fine-tune the pre-trained VILA [19], leveraging its strengths in video comprehension and instruction following. Key modifications include integrating reasoning chains before scoring or ranking and enhancing decision-making with explicit thought processes. This improves result accuracy and the quality of natural language feedback.

We initialize the model with the VILA 13B/40B pre-trained checkpoint and fine-tune it for 5 epochs on our labeled dataset using a learning rate of $2e-5$. Training is distributed across 32 GPUs with a batch size of 4 per GPU. To reduce inconsistencies from scaling and center cropping, we adopt pad training. For improved video understanding, we extract 16 uniformly sampled frames per video while keeping other hyperparameters consistent with VILA’s defaults. This setup balances computational efficiency and model performance, ensuring strong video-text alignment.

4.1.2. T2V Alignment Training

We use a critic model based on diffusion framework to evaluate video quality through semantic and temporal consistency, combining human feedback and objective criteria. We train IPO with DPO and KTO, separately. using a batch size of 128, a learning rate of $2e-5$, and three iterations.

4.2. Results

4.2.1. Quantitative Results

Quantitative results are evaluated using the VBench metric, which measures video generation quality in terms of temporal coherence, semantic alignment, and overall plausibility. As shown in Tab. 1, our experiments reveal that the optimized 2B model outperforms the baseline 5B model across all metrics. The optimized model shows significant improvements in temporal coherence, enhancing frame transi-

tions and minimizing abrupt changes. It also demonstrates stronger semantic alignment, better capturing the intended meaning and context of input prompts. These results highlight the effectiveness of our post-training strategy in addressing key limitations of the baseline model. The overall VBench score further confirms that the optimized 2B model achieves superior video quality while maintaining computational efficiency, making it a practical solution for optimizing smaller-scale models.

4.2.2. Qualitative Results

To further assess the benefits of our approach, we provide qualitative comparisons between the baseline and optimized models. Visual results, shown in Fig. 4, reveal that the optimized 2B model generates videos with better semantic fidelity, accurately capturing the intent of input prompts and their context. It also ensures improved temporal consistency by minimizing artifacts and sudden transitions between frames, common in the baseline outputs. Additionally, the optimized videos exhibit enhanced realism, with fewer incoherent structures and greater plausibility, making them more visually appealing and aligned with human perception. This further demonstrate the effectiveness of IPO.

4.3. Ablation Studies

4.3.1. Incorporating Real Video Data

To explore the impact of real video data during post-training, we integrated real samples into the training process and applied the original diffusion model loss with reinforcement learning objectives. This modification greatly improves generation quality by enhancing temporal coherence, reducing flickering, and strengthening frame consistency. Furthermore, the inclusion of real-world examples boosts semantic alignment, guiding the model to generate more realistic motion dynamics and contextual details.

As shown in Tab. 2, the introduction of real video data (indicated by the inclusion of `sft loss`) leads to measurable improvements across multiple VBench metrics, including temporal flicker, motion smoothness, and aesthetic quality. Notably, the optimized model achieves higher scores in semantic consistency and dynamic degree, indicating a significant enhancement in the realism and coherence of generated videos. These results underscore the effectiveness of integrating real-world data with reinforcement learning to refine video generation outputs, enabling the model to produce videos with superior visual and temporal fidelity.

4.3.2. Comparison of different RL Methods

To evaluate the performance of the proposed online reinforcement learning framework, we conducted experiments using two different feedback alignment methods: Knowledge Transfer Optimization (KTO) and Direct Policy Optimization (DPO). The results, presented in Tab. 4, demonstrate that our framework consistently improves video gen-

Models	Total Score.	Quality Score.	Semantic Score.	Subject Consist.	Background Consist.	Temporal Flicker.	Motion Smooth.	Aesthetic Quality	Dynamic Degree	Image Quality
CogVideoX-2B	80.91	82.18	75.83	96.78	96.63	98.89	97.73	60.82	59.86	61.68
CogVideoX-2B-IPO ₁	81.69	82.87	77.01	96.77	97.01	99.01	97.84	61.55	64.33	62
CogVideoX-2B-IPO ₂	82.42	83.53	77.97	96.81	97.23	99.21	98.03	62.35	68.76	61.77
CogVideoX-2B-IPO ₃	82.74	83.92	78.00	96.79	97.48	99.35	98.17	62.31	69.46	62.87

Table 3. Ablation studies on the iteration number adopted in IPO. The evaluation is performed on VBench.

Method	Quality Score	Semantic Score	Total Score
CogVideoX-2B	80.91	82.18	75.83
CogVideoX-2B-KTO ₁	82.47	83.56	78.08
CogVideoX-2B-DPO ₁	82.42	83.53	77.97

Table 4. Ablation studies on impacts of different preference optimization strategies for IPO: DPO and KTO.

eration quality across multiple metrics, regardless of the specific reinforcement learning method employed. All evaluation metrics across different dimensions are provided in the supplementary materials, further supporting this comprehensive improvement.

Both KTO and DPO lead to significant enhancements over the baseline CogVideoX-2B model, showing improvements in temporal flicker reduction, motion smoothness, and dynamic degree. These results validate the generality and robustness of the proposed online reinforcement learning framework, which effectively integrates human feedback to optimize video generation outputs. For example, the inclusion of either KTO or DPO raises the *Aesthetic Quality* and *Dynamic Degree* metrics compared to the baseline model, underscoring the benefits of aligning the generated outputs with human preferences.

Between the two methods, KTO achieves consistently better performance than DPO across most metrics. Notably, KTO yields a higher *Dynamic Degree* score (68.83 vs. 68.76) and improved *Motion Smoothness* (97.93 vs. 98.03), suggesting that KTO is more effective at producing realistic and temporally coherent videos. Additionally, KTO demonstrates greater stability during training, as evidenced by its higher overall scores across *Subject Consistency* and *Background Consistency*, which measure adherence to semantic and contextual details. These findings highlight the advantages of the KTO method in leveraging multi-step optimization, enabling the generation of more plausible and visually consistent video outputs compared to DPO. This confirms our IPO is flexible to adapt to different optimization methods. In addition, KTO exhibits superior performance and stability, making it a preferred choice.

4.3.3. Effect of Multi-Round Training

The impact of multi-round reinforcement learning is assessed by training models with 1, 2, and 3 rounds of iterative optimization, where a single round represents the traditional offline post-training approach. Results in Tab. 3 show that

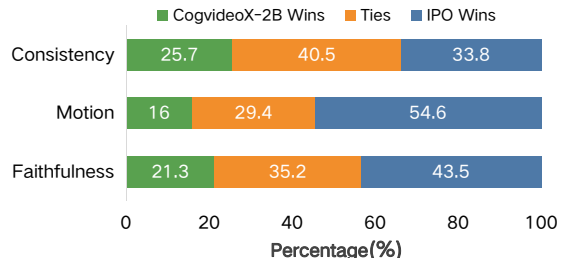


Figure 5. Human evaluation of IPO and CogVideoX-2B.

performance improves with each additional round, as multi-round training better aligns the model with human feedback and refines generation quality. These findings confirm that iterative reinforcement learning effectively enhances both temporal and semantic consistency.

4.4. Human Evaluation

Fig. 5 presents the results of a human evaluation comparing the IPO model with the baseline CogVideo-2B. The result shows that our IPO outperforms the baseline in all dimensions. In the "Consistency" dimension, the two models performed equally in around 40.5 percent of the cases, indicating that the baseline excels in maintaining text consistency. However, in the "Motion" and "Faithfulness" dimensions, the baseline's performance is average, while the IPO model demonstrates a significant improvement, particularly in generating more natural motion and better alignment with the given text. All evaluation metrics across different dimensions are provided in the **supp. materials**

5. Conclusion

In this paper, we present a novel Iterative Preference Optimization framework for improvement video foundation models from the perspective of post training. In particular, IPO collects a human preference dataset and trains a critic model for automatically labeling the generated videos from base model. Given this, IPO efficiently optimizes the base model in an iterative manner. By this way, IPO can effectively align the base model with human preference, leading to enhanced video results in motion smoothness, subject consistency and aesthetic quality, etc. In addition, we adapt IPO with different optimization strategies: DPO and KTO, both achieve impressive improvements. This further verifies the flexibility of IPO. Thorough experiments on VBench demonstrates the efficacy of IPO.

References

- [1] Andreas Blattmann, Robin Rombach, Huan Ling, Tim Dockhorn, Seung Wook Kim, Sanja Fidler, and Karsten Kreis. Align your latents: High-resolution video synthesis with latent diffusion models, 2023. 3
- [2] Tim Brooks, Bill Peebles, Connor Holmes, Will DePue, Yufei Guo, Li Jing, David Schnurr, Joe Taylor, Troy Luhman, Eric Luhman, et al. Video generation models as world simulators. *OpenAI Blog*, 1:8, 2024. 1, 3
- [3] Haoxin Chen, Yong Zhang, Xiaodong Cun, Menghan Xia, Xintao Wang, Chao Weng, and Ying Shan. Videocrafter2: Overcoming data limitations for high-quality video diffusion models, 2024. 3
- [4] Xinyuan Chen, Yaohui Wang, Lingjun Zhang, Shaobin Zhuang, Xin Ma, Jiashuo Yu, Yali Wang, Dahua Lin, Yu Qiao, and Ziwei Liu. Seine: Short-to-long video diffusion model for generative transition and prediction, 2023. 3
- [5] Kevin Clark, Paul Vicol, Kevin Swersky, and David J Fleet. Directly fine-tuning diffusion models on differentiable rewards. *arXiv preprint arXiv:2309.17400*, 2023. 3
- [6] Patrick Esser, Johnathan Chiu, Parmida Atighehchian, Jonathan Granskog, and Anastasis Germanidis. Structure and content-guided video synthesis with diffusion models, 2023. 3
- [7] Kawin Ethayarajh, Winnie Xu, Niklas Muennighoff, Dan Jurafsky, and Douwe Kiela. Kto: Model alignment as prospect theoretic optimization, 2024. 1, 3, 4
- [8] Gen-3. Gen-3. <https://runwayml.com/blog/introducing-gen-3-alpha/>, 2024. 3
- [9] Yuwei Guo, Ceyuan Yang, Anyi Rao, Zhengyang Liang, Yaohui Wang, Yu Qiao, Maneesh Agrawala, Dahua Lin, and Bo Dai. Animatediff: Animate your personalized text-to-image diffusion models without specific tuning. *arXiv preprint arXiv:2307.04725*, 2023. 3
- [10] hailuo. hailuo. <https://hailuoai.video/>, 2024. 1
- [11] Jonathan Ho, Ajay Jain, and Pieter Abbeel. Denoising diffusion probabilistic models. *Advances in neural information processing systems*, 33:6840–6851, 2020. 3, 5
- [12] Jonathan Ho, William Chan, Chitwan Saharia, Jay Whang, Ruiqi Gao, Alexey Gritsenko, Diederik P Kingma, Ben Poole, Mohammad Norouzi, David J Fleet, et al. Imagen video: high definition video generation with diffusion models (2022). *arXiv preprint arXiv:2210.02303*, 2022. 3
- [13] Jonathan Ho, Tim Salimans, Alexey Gritsenko, William Chan, Mohammad Norouzi, and David J Fleet. Video diffusion models. *Advances in Neural Information Processing Systems*, 35:8633–8646, 2022. 3
- [14] Diederik Kingma, Tim Salimans, Ben Poole, and Jonathan Ho. Variational diffusion models. *Advances in neural information processing systems*, 34:21696–21707, 2021. 5
- [15] Weijie Kong, Qi Tian, Zijian Zhang, Rox Min, Zuozhuo Dai, Jin Zhou, Jiangfeng Xiong, Xin Li, Bo Wu, Jianwei Zhang, et al. Hunyuanvideo: A systematic framework for large video generative models. *arXiv preprint arXiv:2412.03603*, 2024. 1, 3
- [16] Kuaishou. Kling. <https://kling.kuaishou.com/en>, 2024. 1, 3
- [17] Jiachen Li, Qian Long, Jian Zheng, Xiaofeng Gao, Robinson Piramuthu, Wenhui Chen, and William Yang Wang. T2v-turbo-v2: Enhancing video generation model post-training through data, reward, and conditional guidance design. *arXiv preprint arXiv:2410.05677*, 2024. 3
- [18] Shufan Li, Konstantinos Kallidromitis, Akash Gokul, Yusuke Kato, and Kazuki Kozuka. Aligning diffusion models by optimizing human utility. *Advances in Neural Information Processing Systems*, 37:24897–24925, 2025. 2, 3
- [19] Ji Lin, Hongxu Yin, Wei Ping, Yao Lu, Pavlo Molchanov, Andrew Tao, Huizi Mao, Jan Kautz, Mohammad Shoeybi, and Song Han. Vila: On pre-training for visual language models, 2023. 7, 3
- [20] Binhui Liu, Xin Liu, Anbo Dai, Zhiyong Zeng, Dan Wang, Zhen Cui, and Jian Yang. Dual-stream diffusion net for text-to-video generation. *arXiv preprint arXiv:2308.08316*, 2023. 3
- [21] Tianqi Liu, Yao Zhao, Rishabh Joshi, Misha Khalman, Mohammad Saleh, Peter J Liu, and Jialu Liu. Statistical rejection sampling improves preference optimization. *arXiv preprint arXiv:2309.06657*, 2023. 3
- [22] Luma. Luma ai. <https://lumalabs.ai/dream-machine>, 2024. 3
- [23] Xin Ma, Yaohui Wang, Gengyun Jia, Xinyuan Chen, Ziwei Liu, Yuan-Fang Li, Cunjian Chen, and Yu Qiao. Latte: Latent diffusion transformer for video generation. *arXiv preprint arXiv:2401.03048*, 2024. 3
- [24] Long Ouyang, Jeffrey Wu, Xu Jiang, Diogo Almeida, Carroll Wainwright, Pamela Mishkin, Chong Zhang, Sandhini Agarwal, Katarina Slama, Alex Ray, et al. Training language models to follow instructions with human feedback. *Advances in neural information processing systems*, 35:27730–27744, 2022. 3
- [25] Mihir Prabhudesai, Anirudh Goyal, Deepak Pathak, and Katerina Fragkiadaki. Aligning text-to-image diffusion models with reward backpropagation, 2024. 3
- [26] Mihir Prabhudesai, Russell Mendonca, Zheyang Qin, Katerina Fragkiadaki, and Deepak Pathak. Video diffusion alignment via reward gradients. *arXiv preprint arXiv:2407.08737*, 2024. 3
- [27] Rafael Rafailov, Archit Sharma, Eric Mitchell, Christopher D Manning, Stefano Ermon, and Chelsea Finn. Direct preference optimization: Your language model is secretly a reward model. *Advances in Neural Information Processing Systems*, 36:53728–53741, 2023. 1, 3, 4, 5
- [28] Rajkumar Ramamurthy, Prithviraj Ammanabrolu, Kianté Brantley, Jack Hessel, Rafet Sifa, Christian Bauckhage, Hannaneh Hajishirzi, and Yejin Choi. Is reinforcement learning (not) for natural language processing: Benchmarks, baselines, and building blocks for natural language policy optimization. *arXiv preprint arXiv:2210.01241*, 2022. 3
- [29] Ludan Ruan, Yiyang Ma, Huan Yang, Huiguo He, Bei Liu, Jianlong Fu, Nicholas Jing Yuan, Qin Jin, and Baining Guo. Mm-diffusion: Learning multi-modal diffusion models for joint audio and video generation, 2023. 3
- [30] Uriel Singer, Adam Polyak, Thomas Hayes, Xi Yin, Jie An, Songyang Zhang, Qiyuan Hu, Harry Yang, Oron Ashual,

- Oran Gafni, et al. Make-a-video: Text-to-video generation without text-video data. *arXiv preprint arXiv:2209.14792*, 2022. 3
- [31] Jascha Sohl-Dickstein, Eric A. Weiss, Niru Maheswaranathan, and Surya Ganguli. Deep unsupervised learning using nonequilibrium thermodynamics. *arXiv: Learning, arXiv: Learning*, 2015. 3
- [32] Jiaming Song, Chenlin Meng, and Stefano Ermon. Denoising diffusion implicit models. *arXiv preprint arXiv:2010.02502*, 2020. 3
- [33] Zhiyu Tan, Xiaomeng Yang, Luozheng Qin, and Hao Li. Vidgen-1m: A large-scale dataset for text-to-video generation, 2024. 5
- [34] Zhiyu Tan, Xiaomeng Yang, Luozheng Qin, Mengping Yang, Cheng Zhang, and Hao Li. Evalalign: Supervised fine-tuning multimodal llms with human-aligned data for evaluating text-to-image models. *arXiv preprint arXiv:2406.16562*, 2024. 3
- [35] Genmo Team. Mochi 1. <https://github.com/genmoai/models>, 2024. 1
- [36] Bram Wallace, Meihua Dang, Rafael Rafailov, Linqi Zhou, Aaron Lou, Senthil Purushwalkam, Stefano Ermon, Caiming Xiong, Shafiq Joty, and Nikhil Naik. Diffusion model alignment using direct preference optimization, 2023. 2, 3, 5
- [37] Jiuniu Wang, Hangjie Yuan, Dayou Chen, Yingya Zhang, Xiang Wang, and Shiwei Zhang. Modelscope text-to-video technical report. *arXiv preprint arXiv:2308.06571*, 2023. 3
- [38] Wenjing Wang, Huan Yang, Zixi Tuo, Huiguo He, Junchen Zhu, Jianlong Fu, and Jiaying Liu. Swap attention in spatiotemporal diffusions for text-to-video generation. *International Journal of Computer Vision*, pages 1–19, 2025. 3
- [39] Chenfei Wu, Lun Huang, Qianxi Zhang, Binyang Li, Lei Ji, Fan Yang, Guillermo Sapiro, and Nan Duan. Godiva: Generating open-domain videos from natural descriptions. *arXiv preprint arXiv:2104.14806*, 2021. 3
- [40] Zhen Xing, Qi Dai, Han Hu, Zuxuan Wu, and Yu-Gang Jiang. Simda: Simple diffusion adapter for efficient video generation, 2023. 3
- [41] Jiazheng Xu, Xiao Liu, Yuchen Wu, Yuxuan Tong, Qinkai Li, Ming Ding, Jie Tang, and Yuxiao Dong. Imagereward: Learning and evaluating human preferences for text-to-image generation. *Advances in Neural Information Processing Systems*, 36:15903–15935, 2023. 3
- [42] An Yang, Baosong Yang, Beichen Zhang, Binyuan Hui, Bo Zheng, Bowen Yu, Chengyuan Li, Dayiheng Liu, Fei Huang, Haoran Wei, et al. Qwen2.5 technical report. *arXiv preprint arXiv:2412.15115*, 2024. 3
- [43] Zhuoyi Yang, Jiayan Teng, Wendi Zheng, Ming Ding, Shiyu Huang, Jiazheng Xu, Yuanming Yang, Wenyi Hong, Xiaohan Zhang, Guanyu Feng, et al. Cogvideox: Text-to-video diffusion models with an expert transformer. *arXiv preprint arXiv:2408.06072*, 2024. 1, 3
- [44] Hangjie Yuan, Shiwei Zhang, Xiang Wang, Yujie Wei, Tao Feng, Yining Pan, Yingya Zhang, Ziwei Liu, Samuel Albanie, and Dong Ni. Instructvideo: Instructing video diffusion models with human feedback, 2023. 3
- [45] Zheng Yuan, Hongyi Yuan, Chuanqi Tan, Wei Wang, Songfang Huang, and Fei Huang. Rrhf: Rank responses to align language models with human feedback without tears. *arXiv preprint arXiv:2304.05302*, 2023. 3
- [46] Qinsheng Zhang, Molei Tao, and Yongxin Chen. gddim: Generalized denoising diffusion implicit models. *arXiv preprint arXiv:2206.05564*, 2022. 3
- [47] Shiwei Zhang, Jiayu Wang, Yingya Zhang, Kang Zhao, Hangjie Yuan, Zhiwu Qin, Xiang Wang, Deli Zhao, and Jingren Zhou. I2vgen-xl: High-quality image-to-video synthesis via cascaded diffusion models. *arXiv preprint arXiv:2311.04145*, 2023. 3
- [48] Tong Zhang. *Mathematical analysis of machine learning algorithms*. Cambridge University Press, 2023. 4
- [49] Yao Zhao, Rishabh Joshi, Tianqi Liu, Misha Khalman, Mohammad Saleh, and Peter J Liu. Slic-hf: Sequence likelihood calibration with human feedback. *arXiv preprint arXiv:2305.10425*, 2023. 3
- [50] Rui Zheng, Shihan Dou, Songyang Gao, Yuan Hua, Wei Shen, Binghai Wang, Yan Liu, Senjie Jin, Qin Liu, Yuhao Zhou, et al. Secrets of rlhf in large language models part i: Ppo. *arXiv preprint arXiv:2307.04964*, 2023. 3

IPO: Iterative Preference Optimization for Text-to-Video Generation

Supplementary Material

A. Human Annotation

Prior to the final manual annotation, we undertook several steps to ensure the quantity, quality, and efficiency of the annotation process. In building the dataset, we focused on the diversity and complexity of prompts, creating annotated data across multiple dimensions and categories. We meticulously selected candidates for the annotation task and provided them with in-depth training sessions. We then designed a user-friendly interface and a comprehensive annotation program to streamline the process. Additionally, we developed a detailed annotation guide that covers all aspects of the task and highlights essential precautions. To further ensure consistency and accuracy among annotators, we conducted multiple rounds of annotation and implemented random sampling quality checks.

A.1. Annotator selection

The effectiveness of annotated data hinges significantly on the capabilities of the individuals responsible for the annotation. As such, at the onset of the annotation initiative, we placed a strong emphasis on meticulously selecting and training a team of annotators to ensure their competence and objectivity. This process entailed administering a comprehensive evaluation to potential candidates, which was designed to gauge their proficiency in ten critical domains: domain expertise, tolerance for visually disturbing content, attention to detail, communication abilities, reliability, cultural and linguistic competence, technical skills, ethical awareness, aesthetic discernment, and motivation.

Given that the models under assessment could generate videos containing potentially distressing or inappropriate material, candidates were informed of this possibility in advance. Their participation in the evaluation was predicated on their acknowledgment of this condition, and they were assured of their right to withdraw at any time. Based on the results of the evaluation and the candidates' professional backgrounds, we sought to form a team that was diverse and well-rounded in terms of expertise and capabilities across the ten assessed areas. Ultimately, we selected a group of 10 annotators—comprising five men and five women, all of whom possessed bachelor's degrees. We conducted follow-up interviews with the selected annotators to reaffirm their suitability for the annotation task.

A.2. Annotation Guideline

When it comes to assessing human preferences in videos, the evaluation process is structured around three fundamental aspects: **semantic consistency**, **motion smoothness**,

and **video faithfulness**. Each of these dimensions is meticulously examined independently to provide a comprehensive understanding of the video's overall quality. **Semantic consistency** ensures that the video's content aligns logically and contextually, while **motion smoothness** evaluates the smoothness and naturalness of movements within the video. **Video faithfulness**, on the other hand, assesses how well the video maintains a realistic and high-quality appearance. By breaking down the evaluation into these distinct yet interconnected aspects, we can achieve a more nuanced and accurate assessment of human preferences in video content.

- **Semantic Consistency** The consistency between the text and the video refers to whether elements such as the topic category (e.g., people or animals), quantity, color, scene description, and style mentioned in the text align with what is displayed in the video.
- **Motion Smoothness** The motion smoothness refers to whether the movements depicted are smooth, coherent, and logically consistent, particularly in terms of their adherence to physical laws and real-world dynamics. This includes evaluating if the actions unfold in a seamless and believable manner, without abrupt or unrealistic transitions, and whether they align with the expected behavior of objects or individuals in the given context.
- **Video Faithfulness** Faithfulness refers to the accuracy and realism of the visual content in the video. It examines whether depictions of people, animals, or objects closely match their real-world counterparts, without unrealistic distortions like severed limbs, deformed features, or other anomalies. High fidelity ensures the visual elements are believable and consistent with reality, enhancing the video's authenticity..

Pointwise Annotation For each dimension, annotators assign one of three ratings:

- **Good:** No observable flaws; fully satisfies the criterion.
- **Normal:** Minor imperfections that do not severely impact perception.
- **Bad:** Significant violations that degrade quality or realism.

Annotations are performed independently across dimensions to avoid bias.

Pairwise Annotation Given two videos \mathcal{V}_A and \mathcal{V}_B , annotators compare them under each dimension:

- For **semantic consistency**, determine which video better aligns with the intended context.

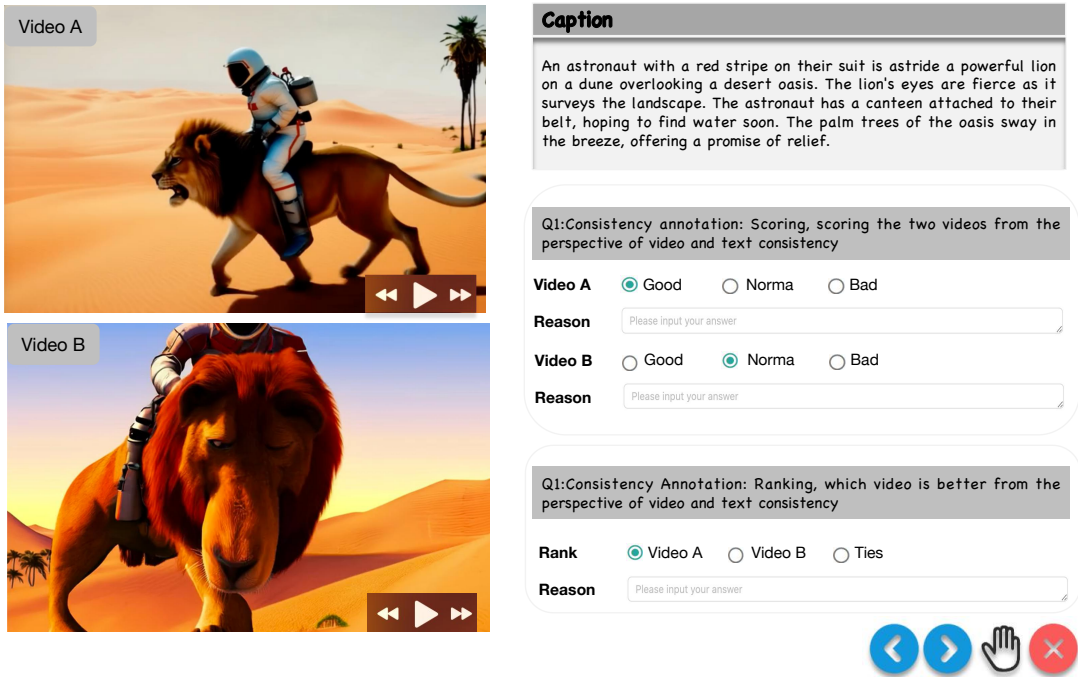


Figure 6. Our user interface presents one sample at a time to annotators, featuring four distinct icons for different functions.

- For **motion smoothness**, identify the video with more natural and continuous motion.
- For **video faithfulness**, select the video exhibiting higher realism and fewer artifacts.

A ranked preference ($\mathcal{V}_A \succ \mathcal{V}_B$ or $\mathcal{V}_B \succ \mathcal{V}_A$) is recorded separately for each dimension. Ties are permitted only if differences are indistinguishable.

A.3. Annotation training and interface

We convened a comprehensive training session centered on our detailed user guidelines to ensure that the annotation team fully comprehends our goals and standards. During the training, we covered the purpose, precautions, standards, workload, and remuneration related to the annotation process. Additionally, we formally communicated to the annotators that the human annotation is strictly for research purposes and that the annotated data might be made publicly available in the future. We reached a mutual agreement with the annotators regarding the standards, workload, remuneration, and intended use of the annotated data. The criteria for assessing video faithfulness, text-video alignment, and motion smoothness are universal, which means that individual standards should not vary significantly. Consequently, we annotated several sample videos using our carefully designed annotation platform to ensure consistency among annotators. An overview of the developed annotation platform is shown in Fig. 6. Through this training, we also equipped the annotators with the necessary knowledge to conduct impartial and detailed human evaluations of video faithfulness,

text-video alignment, and motion smoothness.

B. Additional Quantitative Analysis

B.1. All evaluation dimension results

We present the evaluation metrics of VBench benchmark in 16 different dimensions in the Tab. 5. The results indicate that the performance shows a continuous upward trend in multiple training iterations, indicating that the training is dynamically stable. Although small fluctuations are observed, they can be ignored and will not affect the overall positive progress of the indicator.

B.2. Impact of Critic Model Scale on Accuracy

To evaluate the impact of model scale on critic performance, we experimented with two ViLA-based critic models of 13B and 40B parameters. Fine-tuned on paired and pointwise annotated datasets, these models were assessed on validation tasks, as shown in Tab. 6.

Results show that increasing the model size from 13B to 40B significantly improves accuracy, with the 40B model achieving 80.73% in paired ranking and 86.57% in pointwise scoring—2.92% and 2.62% higher than the 13B model. This suggests that larger critic models better capture human preferences by representing complex multimodal relationships.

Our ablation study further highlights the importance of model scale. While smaller models perform reasonably well, larger models significantly boost accuracy, benefiting

Model	Subject Consistency	Background Consistency	Temporal Flickering	Motion Smoothness	Dynamic Degree	Aesthetic Quality	Imaging Quality	Object Class
CogVideoX-2B	96.78	96.63	98.89	97.73	59.86	60.82	61.68	83.37
CogVideoX-2B-KTO ₁	96.77	97.01	99.01	97.84	64.33	61.55	62	85.41
CogVideoX-2B-KTO ₂	96.81	97.23	99.21	98.03	68.76	62.35	61.77	85.63
CogVideoX-2B-KTO ₃	96.79	97.48	99.35	98.17	69.46	62.28	62.87	85.77

Model	Multiple Objects	Human Action	Color	Spatial Relationship	Scene	Appearance Style	Temporal style	Overall Consistency
CogVideoX-2B	62.63	98.00	79.41	69.90	51.14	24.8	24.36	26.66
CogVideoX-2B-KTO ₁	63.25	98.54	81.67	67.83	54.15	25.13	24.86	27.03
CogVideoX-2B-KTO ₂	63.44	98.97	83.24	70.16	54.35	25.47	26.44	27.37
CogVideoX-2B-KTO ₃	63.51	99.03	82.33	70.23	54.41	25.48	25.39	27.66

Table 5. Quantitative results on video assessment metrics. Display of comparison results between all indicators and baseline on vbench through multiple iterations.

Model Scale	Pairwise Accuracy	Pointwise Accuracy
IPO-Critic-13B	78.41	82.95
IPO-Critic-40B	81.33	85.57

Table 6. Accuracy of Critic Models on Validation Sets Across Different Scales. The critic models used in this study are finetuned from the ViLA[19] multimodal large language model. This table evaluates their performance at different scales (13B and 40B) in terms of accuracy on pairwise and pointwise validation datasets. The results demonstrate that larger model scales yield higher accuracy for both pairwise ranking and pointwise scoring, indicating improved alignment with human preferences as the model size increases.

downstream reinforcement learning tasks. These findings suggest that scaling the critic model is a simple yet effective way to enhance preference alignment and improve video generation quality.

B.3. Impact of Critic Model Size on RL

We conducted a comparative analysis of critic models of different sizes in the iterative preference optimization training process. As shown in Tab. 7, larger critic models provide more precise reward estimations, leading to improved alignment with human preferences. This enhanced reward accuracy contributes to better optimization during preference alignment training, ultimately resulting in superior model performance. Our findings highlight the importance of scaling the critic model to achieve more reliable preference optimization and reinforce the benefits of leveraging larger critic architectures for improved alignment outcomes.

C. Additional Qualitative Comparison

We provide a more detailed qualitative comparison in Fig. 7, which demonstrates the superiority of our model over the baseline. This visualization highlights key improvements in fidelity and overall quality. By comparing outputs side by side, we illustrate the advantages of our model in handling complex scenarios, reinforcing its effectiveness in real-world applications.

D. Societal Impacts

The emergence of advanced text-to-video generation pipelines and optimized training strategies marks a major breakthrough in AI-driven content creation. These innovations significantly lower barriers to video production, making it more efficient, cost-effective, and widely accessible. Industries such as education, entertainment, marketing, and accessibility technology stand to benefit immensely, as creators can generate high-quality videos with minimal effort and resources.

However, alongside these advancements come ethical concerns, particularly regarding potential misuse. One of the most pressing risks is the creation of highly realistic yet misleading content, such as deepfakes, which could be exploited for misinformation, reputational harm, or social manipulation. Additionally, automated video curation may unintentionally reinforce biases present in training datasets, leading to the perpetuation of stereotypes or discriminatory narratives.

On a larger scale, the widespread adoption of AI-driven video generation could disrupt traditional media industries, impacting professions like video editing, animation, and scriptwriting. The proliferation of hyper-realistic AI-generated content also raises concerns about media authenticity, making it increasingly difficult for audiences to distinguish between real and synthetic footage. Furthermore, if access to these technologies remains limited to well-funded organizations, existing digital divides could widen, leaving smaller creators at a disadvantage.

To mitigate these risks, proactive measures must be taken. Implementing transparency features—such as metadata labels to distinguish AI-generated content—can enhance accountability. Ensuring diverse and ethically curated datasets is crucial to reducing bias and promoting fairness in outputs. Policymakers, industry leaders, and researchers must work together to develop regulatory frameworks that balance innovation with ethical responsibility. Additionally, providing educational resources and affordable access to AI tools can help democratize their benefits, preventing technological disparities.

Models	Total Score.	Quality Score.	Semantic Score.	Subject Consist.	Background Consist.	Temporal Flicker.	Motion Smooth.	Aesthetic Quality	Dynamic Degree	Image Quality
CogVideoX-2B	80.91	82.18	75.83	96.78	96.63	98.89	97.73	60.82	59.86	61.68
w/IPO-Critic-13B	82.42	83.53	77.97	96.81	97.23	99.21	98.03	62.35	68.76	61.77
w/IPO-Critic-40B	82.52	83.63	78.07	96.83	97.37	99.19	98.09	62.38	68.92	62.01

Table 7. Evaluate the impact of the critic model on performance, verify the performance of the critic model results for different model sizes of 13B and 40B, a more accurate critic model leads to improved results.

The rapid evolution of generative AI necessitates ongoing ethical oversight. Continuous evaluation of its societal impact, coupled with adaptive safeguards, is essential to minimizing harm while maximizing positive outcomes. Addressing these challenges requires a multidisciplinary approach, fostering a responsible AI ecosystem that empowers creators without compromising ethical integrity.

E. Limitations

While our approach represents a significant advancement in text-to-video generation, several challenges persist. Addressing these issues presents valuable opportunities for future research and development. Below, we outline key limitations and potential solutions:

Computational Constraints Despite improvements in training efficiency, large-scale text-to-video models still demand substantial computational power. This limitation may hinder accessibility, particularly for individuals and organizations with limited resources. Future research should focus on developing lightweight architectures, model compression techniques, and efficient inference strategies to enhance accessibility in resource-constrained environments.

Dataset Representativeness and Cultural Adaptability

The effectiveness of our model is highly dependent on the quality and diversity of its training dataset. While significant efforts were made to curate a representative dataset, certain cultural contexts, niche topics, and underrepresented communities may not be adequately covered. Additionally, biases present in pretraining data could lead to unintended stereotypes or inappropriate outputs. Expanding dataset coverage, improving curation techniques, and integrating fairness-aware training strategies will be crucial to enhancing contextual accuracy and mitigating bias.

Multimodal Hallucination and Interpretability

Since our evaluation models are fine-tuned multimodal large language models (MLLMs), they are susceptible to hallucination—generating content that appears plausible but is factually incorrect or cannot be inferred from the input text and images. Furthermore, MLLMs inherit biases from their pretraining data, which may lead to inappropriate responses. While careful curation of supervised fine-tuning (SFT) data

helps alleviate these issues, they are not fully resolved. In addition to these concerns, MLLMs also suffer from opacity, interpretability challenges, and sensitivity to input formatting, making it difficult to understand and control their decision-making processes. Enhancing model explainability and robustness remains a crucial area for future research.

Human Annotation Limitations

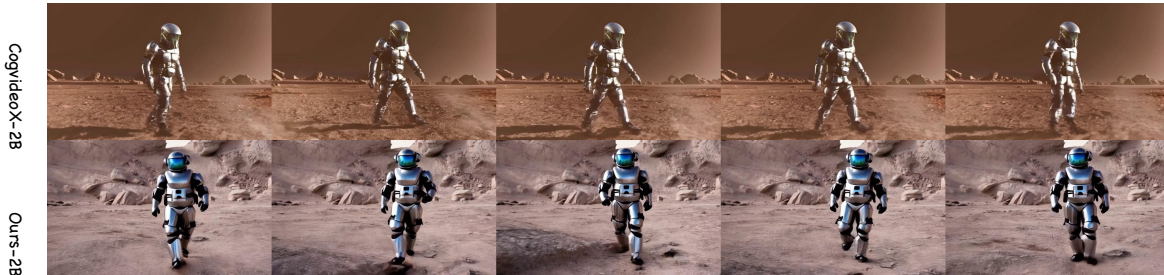
Human evaluation plays a critical role in assessing model performance, but it is inherently subjective and influenced by annotator biases, perspectives, and inconsistencies. Errors or noisy labels may arise during annotation, potentially affecting evaluation reliability. To address this, we conducted multiple rounds of trial annotations and random sampling quality inspections to improve inter-annotator consistency. Additionally, we designed user-friendly annotation guidelines and interfaces to streamline the process and enhance accuracy. However, variations in annotation methodologies across different platforms and annotators can still lead to discrepancies, limiting the generalizability of our results. Moreover, human annotation remains time-consuming and resource-intensive, constraining scalability. Future efforts could explore semi-automated evaluation approaches or crowd-sourced methods to improve efficiency while maintaining quality.

Ethical Considerations and Regulatory Compliance

Ensuring responsible AI deployment remains an ongoing challenge, even with safeguards in place to prevent misuse. The rapid advancement of AI-generated media demands continuous revisions to ethical policies and regulatory frameworks. Proactively engaging with policymakers, industry leaders, and researchers is crucial for developing guidelines that uphold accountability, transparency, and fair usage. Embedding metadata or digital watermarks in AI-generated content can improve traceability and help differentiate synthetic media from authentic sources. Furthermore, raising public awareness and education on AI-generated content help users recognize potential risks. Developers should prioritize responsible AI innovation by ensuring algorithmic fairness while minimizing bias. Additionally, fostering cross-industry collaboration and promoting global standards will contribute to a more secure and trustworthy AI ecosystem.



A silver flying motorcycle with a sleek design and a powerful engine zooms through a city. The motorcycle's rider wears a helmet and leather jacket as they navigate through traffic.



A man dressed as a robot astronaut walks across a barren, rocky landscape on a distant planet. His sleek, metallic suit glimmers under the dim light of a distant sun, and his helmet reflects the alien terrain. He strides purposefully, leaving faint footprints in the dust, with a sense of determination and exploration. The desolate environment, dotted with boulders and sparse vegetation, enhances the otherworldly atmosphere of his journey.



A rugged worker in a plaid shirt and denim jeans leads a strong, chestnut-colored horse along a dusty, rural path. The horse, adorned with a simple leather harness, walks steadily beside the worker, who holds the reins with a firm yet gentle grip. The scene is set in the late afternoon, with warm sunlight casting long shadows and highlighting the textures of the dirt road and the surrounding countryside. The worker's weathered face and the horse's powerful presence convey a sense of steadfast determination and mutual respect.



A young girl in a futuristic spacesuit runs across a vast, icy landscape on a distant planet, with a towering mammoth-like creature beside her. The mammoth's massive, shaggy form and long tusks contrast with the stark, alien environment. The sky above is a deep, star-filled space, with distant planets and nebulae visible. The girl's determined expression and the mammoth's steady pace convey a sense of adventure and discovery in this otherworldly setting.

Figure 7. **Enhanced qualitative comparison.** We conduct a qualitative comparison between CogVideo-2B and IPO-2B to evaluate their performance